Origin of phonon anomalies in La_2CuO_4

Claus Falter, Michael Klenner, and Georg A. Hoffmann
Institut für Theoretische Physik II–Festkörperphysik, Universität Münster, Wilhelm-Klemm-Strasse 10, 48149 Münster, Germany

Qiang Chen
Department of Applied Mathematics and Physics, 33-109, Beijing University of Aeronautics and Astronautics, 100083 Beijing, People's Republic of China

(Received 22 April 1996; revised manuscript received 22 July 1996)

The experimentally observed softening of the oxygen breathing mode at the X point, O_X^B, and of a second CuO bond stretching mode of Δ_1 symmetry at the wave vector $\mathbf{q}=(0.5,0,0)$ in the doped metallic phase of La-Cu-O is investigated and shown to be driven by long-range, nonlocal electron-phonon interaction effects of monopole charge-redistribution type. The amplification of softening for both modes by about 1 THz, recently found in inelastic neutron scattering for an optimally doped $La_{1.85}Sr_{0.15}CuO_4$ probe as compared with an underdoped $La_{1.9}Sr_{0.1}CuO_4$ crystal is explained by the growing importance of the more extended orbitals in the charge response in particular at the Cu ion. Such an enlarged contribution of the more extended orbitals leads to a reduction of the dominant self-interaction, U, of the electrons mainly at the Cu and allows for an enhancement of the monopole charge redistributions whose magnitude determines the softening of the phonon modes. The existence of a specific mixture of localized and more extended states at the Fermi energy is crucial for the appearance of the strong nonlocal electron-phonon coupling of ionic origin and for the reinforcement of the phonon mediated part of pairing in the high-temperature superconductors. [S0163-1829(97)02005-5]

The details of the theoretical description of the electronic density response developed in order to investigate local and nonlocal electron-phonon interaction (EPI) effects in the high-temperature superconductors (HTSC's) can be found in Refs. 1 and 2. Within this formulation the displacement-induced change of the electronic density, i.e., the vectorfield $\mathbf{P}^{\mathbf{a}}_{\alpha}(\mathbf{r})$, is given by

$$\mathbf{P}^{\mathbf{a}}_{\alpha}(\mathbf{r})=\left.\frac{\partial\rho(\mathbf{r})}{\partial\mathbf{R}^{\mathbf{a}}_{\alpha}}\right|_0=[\mathbf{P}^{\mathbf{a}}_{\alpha}(\mathbf{r})]_{\mathrm{RIM}}-\sum_{\mathbf{b}\kappa}\rho_{\kappa}(\mathbf{r}-\mathbf{R}^{\mathbf{b}}_{\kappa})\mathbf{X}^{\mathbf{ba}}_{\kappa\alpha}. \quad (1)$$

$\mathbf{a}$ denotes the unit cell, α the sublattice, $\mathbf{R}^{\mathbf{a}}_{\alpha}=\mathbf{R}^{\mathbf{a}}+\mathbf{R}^{\alpha}$ gives the location of the ions in the crystal, and $\rho(\mathbf{r})$ is the electron density at the space point $\mathbf{r}$. The derivative has to be taken at the equilibrium positions of the ions. The index ''RIM'' in Eq. (1) means ''rigid ion model'' and indicates the rigid part of the density response. The $\mathbf{R}^{\mathbf{b}}_{\kappa}$ describe the localization centers of the charge fluctuations (CF's) of type κ in the unit cell, i.e., the ionic shells in a dominantly ionic system.

Because the term (phonon-induced) charge fluctuation, which is used here in the sense as introduced for example in Ref. 3, may be misleading to some readers we shall recall its meaning. First of all its rigorous mathematical definition in terms of the appropriate quantities of (linear) response theory is provided by combining Eqs. (2), (6), and (7); see below. In a physical picture the CF's considered here are charge rearrangements of monopole type due to the forces as induced by the displaced ions in a certain phonon mode, i.e., one can imagine that electronic charge is added or taken away from the outer shells of the overlapping ions making up the crystal due to these forces. During such an electronic polarization process charge can be transferred between the different shells of a certain ion (for example in case of the copper ion where we allow for CF's of $3d$, $4s$, and $4p$ type) or equally well between the shells of different ions (say between the copper and the oxygen). If the adiabatic approximation applies to the calculation of the phonon frequencies, the CF's are *static* quantities because the electronic polarizability Π in Eq. (2) can be treated in its static (frequency independent) approximation. However, in a nonadiabatic treatment of the phonons, which seems to be essential for certain modes propagating along the c axis in the HTSC's, Π must be used in its full frequency dependent form, i.e., dynamical screening applies. In this case the charge rearrangements denoted as CF's become *dynamical* quantities (plasmons) and one enters the phonon-plasmon scenario discussed in Refs. 2 and 4.

The densities $\rho_{\kappa}(\mathbf{r})$ are the form factors of the CF's, i.e., they determine the shape and the degree of spatial extension of the change in the density associated with the different CF's being admitted in a particular model. In the present model we allow for La $5d$, Cu $3d$, $4s$, $4p$, and O $2p$ CF's. Consistent with these electronic degrees of freedom we calculate the electronic polarizability Π in the tight-binding representation from the tight-binding analysis of the first principles electronic band structure for LaCuO as given in Ref. 5 leading altogether to a 31-band model. Our result for the recalculated tight-binding band structure is shown in Fig. 1; compare with Fig. 2 in Ref. 5. The ρ_{κ} are approximated by the spherically averaged orbital density of the La $5d$, Cu $3d$, $4s$, $4p$, and O $2p$ shell, respectively.

The quantity $\mathbf{X}$ in Eq. (1) gives the self-consistent reaction of the CF's in response to an ion displacement. In a physical picture the second term in Eq. (1), including $\mathbf{X}$, contains the electronic polarization nonlocally induced by the phonons whose degree of localization obviously varies with doping in the HTSC's as can be seen by our discussion of the phonon anomalies below. In turn this charge polariza-

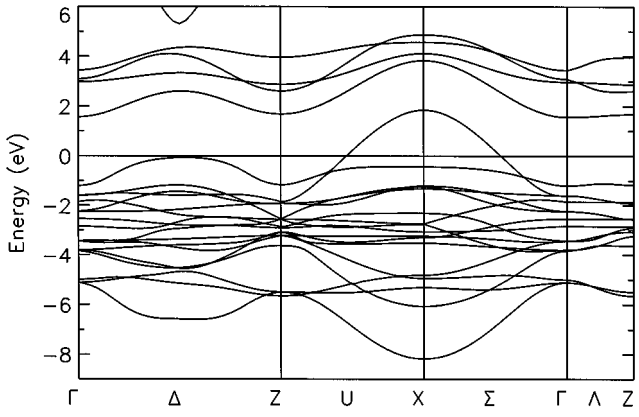

FIG. 1. Electronic band structure of La_2CuO_4 in the 31 band tight-binding model fitted to the first-principles LAPW band structure. The Fermi energy E_F is taken as the zero of the energy.

tion is coupled back to the ions leading to an additional contribution to the ionic displacements besides the coupling effect resulting from the first term in Eq. (1) arising from local EPI. The second term in Eq. (1) describes nonrigid as well as nonlocal phonon-induced redistributions of the density. The latter are clearly nonrigid because they are beyond the contribution from the rigid displacement of the ions [first term in Eq. (1)]. But they are also nonlocal because the displacement of an ion $(\mathbf{a}\alpha)$ may induce CF's $(\mathbf{b}\kappa)$ on a different ion, say $(\mathbf{b}\beta)$. For example in the planar breathing mode, O_X^B, discussed below, the moving O_{xy} ions induce CF's on the Cu ion staying at rest; see the corresponding contour plots below. Of course, there may be also a local contribution, namely, if there are CF's on the displaced ion itself. The same reasoning applies to the phonon induced changes of the crystal potential at the ion sites (nonlocal EPI).

X can be expressed in compact matrix-notation using linear response theory as

$$\mathbf{X}=\Pi\varepsilon^{-1}\mathbf{B} \quad \text{with} \quad \varepsilon=1+\tilde{V}\Pi. \tag{2}$$

ε denotes the dielectric function and **B** yields the interaction between the CF's and the displaced ions. The effective interaction between the electrons, $\tilde{V}$, and the quantity **B** can be calculated from the ionic self-energies and the pair potentials between the ions by allowing for variable occupation of the electron orbitals. For the exact definition of $\tilde{V}$ and **B** in terms of the derivatives of the crystal energy in pair-potential-approximation with respect to the ion coordinates and the charge fluctuation degrees of freedom, respectively; see, e.g., Ref. 4.

$[\mathbf{P}_\alpha^{\mathbf{a}}(\mathbf{r})]_{\mathrm{RIM}}$ in Eq. (1) constitutes the explicit change of the density due to the movement of the rigid ions and approximates the local part of the EPI. The method of Gordon and Kim[6] is used to determine the pair potentials from the ionic densities which on the other hand are obtained from a modified version of the Herman-Skillman program taking into account averaged self-interaction corrections.[7] Moreover, the ionic densities are calculated consistently with effective ionic charges as obtained from the orbital occupation numbers resulting from a tight-binding analysis of the electronic band structure in the 31-band model. Including additionally covalence corrections for certain pair potentials such a model serves as a reference system for the insulating phase of the HTSC's and leads to good results for the structural parameters and the phonon dispersion of insulating LaCuO.[2]

For a description of the doped metallic phase of the HTSC's the nonlocal contributions of the electronic density response and the EPI [second term in Eq. (1)] are also taken into account. In other words, the metallic character of bonding and the metallic compressibility is established in our theory by the more or less localized CF's on the outer electron shells of the ions (together with the corresponding electronic polarizability Π) which are calculated in agreement with the ionic model making the occupation numbers of the orbitals variable. Ultimately, the dynamical matrix $t(\mathbf{q})$ can be decomposed analogously to $\mathbf{P}_\alpha^{\mathbf{a}}$ from Eq. (1) as

$$t_{ij}^{\alpha\beta}(\mathbf{q})=[t_{ij}^{\alpha\beta}(\mathbf{q})]_{\mathrm{RIM}}-\frac{1}{\sqrt{M_\alpha M_\beta}}\sum_\kappa [B_i^{\kappa\alpha}(\mathbf{q})]^* X_j^{\kappa\beta}(\mathbf{q}) \tag{3}$$

[$B_i^{\kappa\alpha}(\mathbf{q})$ and $X_j^{\kappa\beta}(\mathbf{q})$ are the Fourier transform of $B_{\kappa\alpha}^{\mathbf{oa}}{}_{i}$ and $X_{\kappa\beta}^{\mathbf{ob}}{}_{j}$, respectively; M_α denotes the ion mass] and the phonon-induced change of the electron density in the mode $(\mathbf{q}\sigma)$ is given by

$$\delta\rho(\mathbf{r},\mathbf{q}\sigma)=\sum_{\mathbf{a},\alpha,i} P_{\alpha}^{\mathbf{a}}{}_{i}(\mathbf{r})u_{\alpha}^{\mathbf{a}}{}_{i}(\mathbf{q}\sigma). \tag{4}$$

Here $\mathbf{P}_\alpha^{\mathbf{a}}$ is expressed by Eq. (1) and $\mathbf{u}_\alpha^{\mathbf{a}}(\mathbf{q}\sigma)$ means the amplitude of the displacement of an ion $(\mathbf{a}\alpha)$ in the mode $(\mathbf{q}\sigma)$ with frequency $\omega_\sigma(\mathbf{q})$ and polarization vector $\mathbf{e}^\alpha(\mathbf{q}\sigma)$,

$$\mathbf{u}_\alpha^{\mathbf{a}}(\mathbf{q}\sigma)=\left(\frac{\hbar}{2M_\alpha\omega_\sigma(\mathbf{q})}\right)^{1/2}\mathbf{e}^\alpha(\mathbf{q}\sigma)e^{i\mathbf{q}\cdot\mathbf{R}_\alpha^{\mathbf{a}}}. \tag{5}$$

The experimental results for the oxygen dominated high-frequency phonon branches Δ_1 and Σ_1 in La-Cu-O to be discussed in this paper have been reproduced from Ref. 8 in Fig. 2. They show the characteristic softening for O_X^B [endpoint of the $\Sigma\sim(1,1,0)$ direction] and even more strongly for a second CuO bondstretching mode at $\mathbf{q}=(0.5,0,0)$. The latter is called $\Delta_1/2$ in the following. Also shown are the displacement patterns for O_X^B and $\Delta_1/2$ and the observed linewidths of the modes together with the experimental resolution. Note that both O_X^B and $\Delta_1/2$ involve also a small symmetric displacement of the apex oxygens not displayed in the figure.

Concerning the softening of O_X^B and $\Delta_1/2$ new neutron scattering experiments show for an optimally doped $La_{1.85}Sr_{0.15}CuO_4$ crystal that these modes further decrease in frequency by about 1 THz as compared with the results for the $La_{1.9}Sr_{0.1}CuO_4$ probe given in Fig. 2.[9] This leads for the Σ_1 branch to a downward curved dispersion when approaching the X point from Γ along the Σ direction, in contrast to the upward curved data for the underdoped crystal shown in Fig. 2, and for the Δ_1 branch to a deeper minimum at $\Delta_1/2$. Exactly these features, even quantitatively, are obtained by our calculations using the 31-band model in the

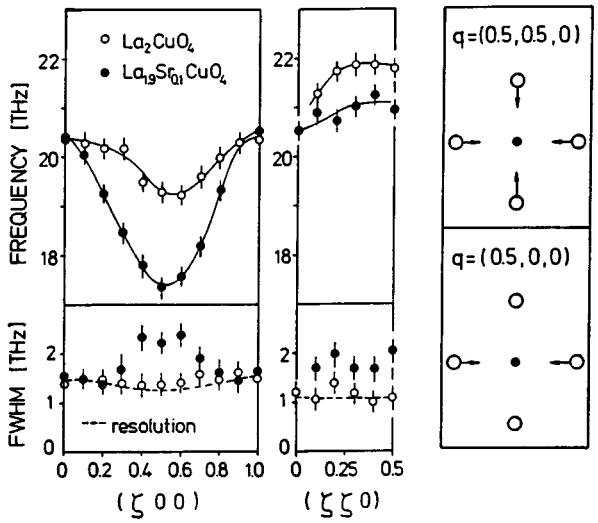

FIG. 2. Experimental results for the highest Δ_1 and Σ_1 branches in insulating La_2CuO_4 and metallic $La_{1.9}Sr_{0.1}CuO_4$ as reproduced from Ref. 8. The bottom part of the left figure shows the observed linewidths together with the experimental resolution. Further given are the displacement patterns for the O_X^B and the $\Delta_1/2$ mode in the CuO plane.

expression for the polarizability and allowing in a consistent manner for CF's of La $5d$, Cu $3d$, $4s$, $4p$, and O $2p$ type; see the full curve in Fig. 3.

The softening of these modes is absent in the ionic reference model where only local EPI effects in terms of rigidly shifted ionic densities ($[\mathbf{P}_\alpha^{\mathbf{a}}(\mathbf{r})]_{\mathrm{RIM}}$ in Eq. (1)) are taken into account.[1,2] Comparing with the present calculation the characteristic phonon anomalies seen for the metallic phase consequently arise because of the strong nonlocal EPI effects of charge fluctuation type embodied in the second term of Eq.

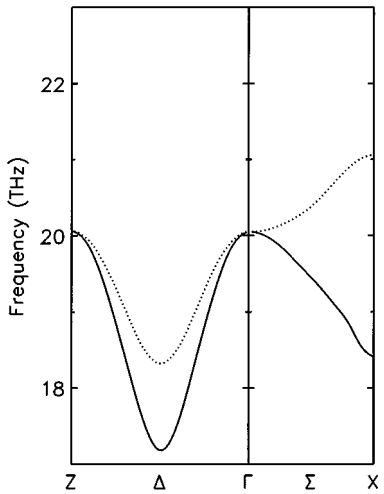

FIG. 3. Calculated results (full curves) for the highest Δ_1 and Σ_1 branch for metallic LaCuO using the 31-band model from the tight-binding analysis (Ref. 5) of the first principles electronic band structure for the electronic polarizability Π and allowing for La $5d$, Cu $3d$, $4s$, $4p$, and O $2p$ charge fluctuations. The Fermi energy is chosen at the van Hove singularity. The dotted curves represent calculations where the more extended $4s$ and $4p$ electronic degrees of freedom at the Cu ion have been suppressed, as compared to the complete calculation displayed by the full curves.

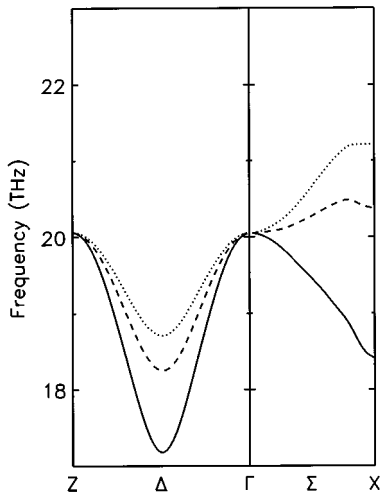

FIG. 4. Full curves are the same as in Fig. 3. The broken and dotted curves represent calculations where all the Cu on-site Coulomb-XC interactions (d-d, s-s, p-p, s-d, p-d, p-s) have been increased by a factor 1.5 and 2.0 as compared to their calculated values (full curves), respectively.

(1). An earlier model calculation for the insulating phase of La-Cu-O allowing additionally to the rigid charge response of the purely ionic model also for nonlocal CF's restricted, however, by the gap in the energy spectrum of the electrons[1] already indicates a weak minimum for $\Delta_1/2$ but an upward dispersion for the Σ_1 branch similar as the experimental results for the insulator in Fig. 2. Besides the LO-TO splitting at Γ the dispersion curves from the insulator model in Ref. 1 also resemble those represented as dotted lines in Fig. 3. Here we have arbitrarily omitted the more extended $4s$ and $4p$ electronic degrees of freedom at the Cu ion as compared to the complete calculation including these electron states and represented by the full lines in Fig. 3. This leads to a significant reduction of the CF's at the Cu because the only charge fluctuating states left at the Cu ion now belong to the strongly localized d electrons, a situation most adequate for the insulating phase and for the underdoped phase where in the latter case, however, delocalization starts growing. Simultaneously with the suppression of the CF's by localization an increase of the corresponding phonon frequencies related to the metal-insulator transition as seen in both, the experiments and the calculations, follows quite naturally. Moreover, in the insulating and less strongly in the underdoped phase we can expect a growing on of the on-site Coulomb-XC interactions because of the importance of the localized Cu $3d$ states. In order to investigate the influence of such a localization effect on the CF's and the phonon dispersion we have enlarged in a model calculation all the Cu on-site Coulomb-XC interactions by a factor 1.5 (see the broken curves in Fig. 4) and by 2.0, respectively (see the dotted curves in Fig. 4). As a result we find a strong suppression of the Cu $3d$, $4s$, and $4p$ CF's generated by the moving oxygen ions via nonlocal EPI and a corresponding increase of the phonon frequencies which is also seen in the experiments for the underdoped probe and the insulating one. Note that for symmetry reasons there are no CF's at the moving oxygen ions in O_X^B. However, in the $\Delta_1/2$ mode the O_y are silent in case the O_x are moving and vice versa. Thus

in addition to the CF's at the Cu ion also CF's at the silent oxygens become possible. This fact leads to an additional source for softening in case of $\Delta_1/2$ as compared to O_X^B where only CF's at the silent Cu ions are possible. For completeness it should be remarked that there are also small CF's at the apex oxygens and the La ions for $\Delta_1/2$ and O_X^B.

The physical reason for the enhanced screening and the corresponding softening for O_X^B and $\Delta_1/2$ in case of the optimally doped crystal can be extracted from our calculations to be related to the large contributions to the CF's from the Cu $4s$ and $4p$ orbitals. The latter represent in an orbital picture the more extended part of the electron states and the density response while the Cu $3d$ states represent the localized more correlated part of the electronic structure leading in our calculation to large on-site Coulomb-XC interactions, U, in contrast to the on-site U's for Cu $4s$ and $4p$ (and also for La $5d$ and O $2p$) being much smaller. The phonon-induced CF's are given by

$$\delta\zeta_\kappa^{(\mathbf{q}\sigma)} = -\sum_{\alpha,i}\left(\frac{\hbar}{2M_\alpha\omega_\sigma(\mathbf{q})}\right)^{1/2} e_i^\alpha(\mathbf{q}\sigma)X_i^{\kappa\alpha}(\mathbf{q})e^{i\mathbf{q}\cdot\mathbf{R}^\kappa}, \qquad (6)$$

and in terms of these quantities the corresponding change of the electron density are given by Eqs. (1), (4), and (5) can be decomposed into a local rigid-ion part and a nonlocal charge-fluctuation contribution

$$\delta\rho(\mathbf{r},\mathbf{q}\sigma) = [\,\delta\rho(\mathbf{r},\mathbf{q}\sigma)\,]_{\mathrm{RIM}} + \sum_{\mathbf{a}\kappa}\rho_\kappa(\mathbf{r}-\mathbf{R}_\kappa^{\mathbf{a}})\,\delta\zeta_\kappa^{(\mathbf{q}\sigma)}e^{i\mathbf{q}\cdot\mathbf{R}^a}. \qquad (7)$$

The CF's at the Cu ion for the two modes are (in units of 10^{-3} electrons) as follows:

$$\Delta_1/2 \rightarrow \text{Cu } 3d\ 14.34,\ \text{Cu } 4s\ 10.41,\ \text{Cu } 4p\ 6.97;$$

$$O_X^B \rightarrow \text{Cu } 3d\ 15.92,\ \text{Cu } 4s\ 20.69,\ \text{Cu } 4p\ 9.4.$$

Thus a major part of the CF's is due to the more extended states, despite their weak occupation ($4s^{0.3}$,$4p^{0.24}$) as obtained for the electron configuration from a tight-binding analysis of the first principles electronic band structure; see Ref. 2. An impression for the degree of localization (extension) for the different Cu states involved can be extracted from Fig. 5 where the orbital form factors ρ_κ (times $4\pi r^2$) are plotted.

Concerning the magnitude of the CF's it is quite interesting to compare the situation in the HTSC's with that in a typical classical ionic oxide material. The calculated CF's for $\Delta_1/2$ and O_X^B, i.e., for a typical HTSC, are about a factor 10 larger than the CF's recently obtained for MgO (Ref. 10) for the longitudinal optical mode at the L point of the Brillouin zone where the oxygen ions are moving at about the same frequency (as in case of $\Delta_1/2$ or O_X^B) against the silent Mg ions.

The enhanced screening effect brought about by the growing importance of the more extended states in case of the optimal doped probe can also be discussed at least qualitatively in a simpler model with a reduced set of electronic degrees of freedom, like the one proposed in Ref. 1 where CF's are only allowed for the Cu $3d$ and the $O_{x,y}$ $2p$ states of the ions in the CuO plane. The contribution of the more extended electronic degrees of freedom not explicitly considered in this model results in renormalized (screened) on-site Coulomb-XC interactions, mainly at the Cu ion. Using such reasoning, the anomalous softening for O_X^B and $\Delta_1/2$ now seen in the experiments and in Fig. 3 already has been predicted in Ref. 1.

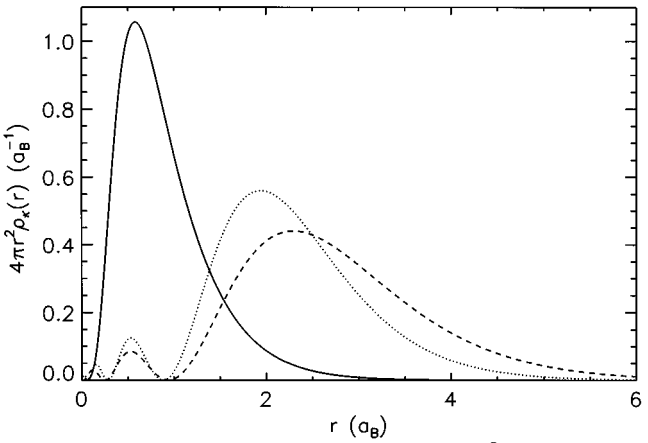

FIG. 5. Charge density form factors (times $4\pi r^2$) for the Cu ion as calculated for the electron configuration ($3d^{9.24}$, $4s^{0.3}$, $4p^{0.24}$) determined from a tight-binding analysis of the first principles band structure of La-Cu-O; see Ref. 2. r radial distance in units of a_B. $3d$ (full curve); $4s$ (dotted curve); $4p$ (broken curve).

Further experimental evidence other than phonons for the growing importance of the delocalized states in case of the optimal doped probe comes from optical conductivity measurements; see, e.g., Ref. 11, which clearly demonstrate that in the high-T_c regime an itinerant-carrier contribution develops in the conductivity spectrum.

Figures 6 and 7 display our calculated results of the phonon-induced charge density redistribution for $\Delta_1/2$ and O_X^B according to Eqs. (6) and (7). Figure 6(a) shows the contribution of the nonlocal part and Fig. 6(b) the total one. As mentioned shortly the moving O_x generates for $\Delta_1/2$ via nonlocal EPI CF's at the silent Cu and O_y ions resulting in a charge transfer within and between the CuO chains. The charge redistribution from the local EPI essentially leads to dipolar charges at the moving ions; see Fig. 6(b). In case of the oxygen breathing mode O_X^B (only the nonlocal contribution is shown in Fig. 7) the moving $O_{x,y}$ induce CF's at the Cu and we obtain an electronic charge transfer from that Cu ion where the CuO bonds are compressed to the Cu where the CuO bonds are stretched. On the whole, negatively charged stripes of ions (for O_X^B along the diagonals in the CuO plane and for $\Delta_1/2$ along the x or y axes, respectively) alternate with positively charged chains of ions. These localized oppositely charged arrays generated nonlocally by the lattice deformation in the particular phonon mode are energetically stabilized by their mutual Coulomb interactions.

In summary our calculations have shown that the electronic state in LaCuO and most probably also in the other Cu based HTSC's consists of a specific mixture of hybridized localized and delocalized components. The comparatively large localized Cu $3d$ part (see for example the values for the Cu $3d$ CF's above) is crucial for the appearance of the strong nonlocal ionic EPI effects of CF type found in our calculations. With only delocalized states present the phonon-

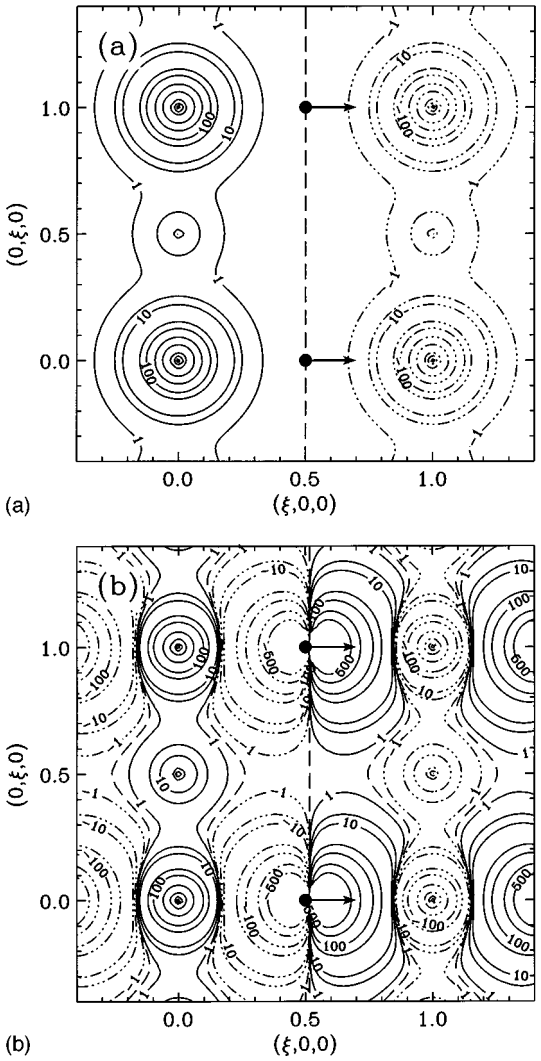

FIG. 6. Contour plot of the charge-density redistribution $\delta\rho$ (scaled by a factor 10^4) within the 31-band model according to Eq. (7) induced by the $\Delta_1/2$ mode. Part (a) of the figure gives the nonlocal contribution of the charge fluctuations [second term in Eq. (7)] and part (b) displays the total change in the electronic density including the local part from the rigidly shifted ions. The moving O_x ions are indicated as dots. $\delta\rho>0$ (full lines) means that electrons are accumulated in the particular region of space. Units are in electrons/a_B^3.

induced changes of the potential an electron feels in the crystal would be very effectively screened and local EPI would dominate as in case of conventional metals and superconductors. In the optimally doped LaCuO crystal we find for the phonon anomalies O_X^B and $\Delta_1/2$ an enhanced contribution to the screening from the more extended orbitals which on the other hand still can experience the strong nonlocal ionic coupling to the ions. This would not be possible in a conventional homogeneous electron gas metal with the carriers only in delocalized states. In case the more extended electronic component becomes sufficiently large, which most likely will happen in the overdoped regime of the HTSC's, the importance of the nonlocal EPI effects is diminished. Moreover, their significant contribution to the phonon mediated part of the pairing mechanism can be expected to be strongly reduced different from the situation found for the optimally doped crystal.

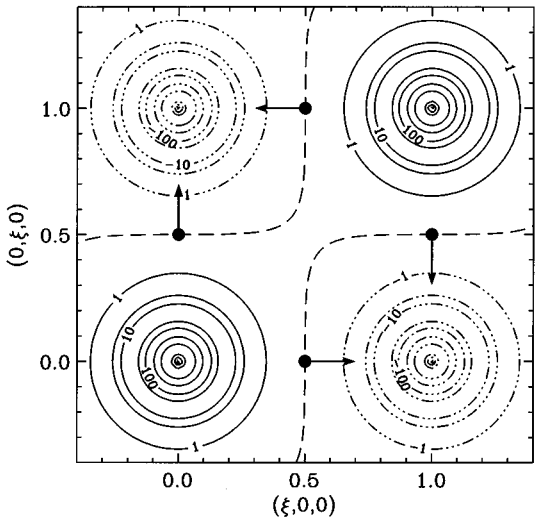

FIG. 7. Contour plot of the nonlocal contribution to the charge density redistribution $\delta\rho$ (scaled by a factor 10^4) within the 31-band model according to Eq. (7) induced by the O_X^B mode. The moving O_x and O_y ions are represented as dots. $\delta\rho>0$ (full lines) means that electrons are accumulated in the particular region of space. Units are in electrons/a_B^3.

Finally, these strong nonlocal EPI effects will lead to modifications of the quasiparticle properties in the HTSC's like band structure renormalization and lifetime effects neglected in our calculation for the electronic polarizability. Thus quite different from the low-T_c materials an unusual quasiparticle transport and optical response caused by the strong nonlocal coupling of the electrons to the phonons will be a consequence. In particular inelastic charge scattering from thermal phonons nonlocally and partly nonadiabatically coupled to the electrons (c-axis phonons) will become important.[2] Furthermore, the low-lying c-axis plasmon found in our recent calculations[2,4,12] mixing with certain c-axis phonons of appropriate symmetry is very likely to become strongly damped or even overdamped by the strong nonlocal EPI.

We thank Dr. L. Pintschovius for communicating his experimental results prior to publication. Financial support by the Deutsche Forschungsgemeinschaft is gratefully acknowledged.

[1] C. Falter, M. Klenner, and W. Ludwig, Phys. Rev. B **47**, 5390 (1993).

[2] C. Falter, M. Klenner, and G. A. Hoffmann, Phys. Rev. B **52**, 3702 (1995).

[3] S. K. Sinha, in *Dynamical Properties of Solids*, edited by G. K Horton and A. A. Maradudin (North-Holland, Amsterdam, 1980), Vol. 3, pp. 1–93.

[4] C. Falter and M. Klenner, Phys. Rev. B **50**, 9426 (1994).

[5] M. J. De Weert, D. A. Papaconstantopoulos, and W. E. Pickett, Phys. Rev. B **39**, 4235 (1989).

[6] R. G. Gordon and Y. S. Kim, J. Chem. Phys. **56**, 3122 (1972).
[7] J. P. Perdew and A. Zunger, Phys. Rev. B **23**, 5048 (1981).
[8] L. Pintschovius and W. Reichardt, in *Physical Properties of High Temperature Superconductors IV*, edited by D. M. Ginsberg (World Scientific, Singapore, 1994), pp. 295–374.
[9] L. Pintschovius (private communication).
[10] C. Falter, G. A. Hoffmann, and M. Klenner, Phys. Rev. B **53**, 14 917 (1996).
[11] S. Uchida, T. Ido, H. Tagaki, T. Arima, Y. Tokura, and S. Tajima, Phys. Rev. B **43**, 7942 (1991).
[12] C. Falter, M. Klenner, and Q. Chen, Phys. Rev. B **48**, 16 690 (1993).